Microelectronics Reliability 51 (2011) 107–112

Contents lists available at ScienceDirect

Microelectronics Reliability

journal homepage: www.elsevier.com/locate/microrel

Influence of bonding process parameters on chip cratering and phase formation of Cu ball bonds on AlSiCu during storage at 200 °C

S. Schmitz *, M. Schneider-Ramelow, S. Schröder

Fraunhofer Institute for Reliability and Microintegration, Berlin, Germany

ARTICLE INFO

Article history:
Received 31 January 2010
Received in revised form 16 July 2010
Accepted 16 July 2010
Available online 21 August 2010

ABSTRACT

Wire bonding remains the predominant interconnection technology in microelectronic packaging. Over the last 3 years a significant trend away from Au and towards Cu wire bonding has become apparent. This has been due to general efforts to lower manufacturing costs and price increases for raw materials like Au. Although much research has been carried out into wire bonding over recent decades, most has focused on Au ball/wedge bonding. The results of this research have shown that bonding parameters, bonding quality and reliability are closely interconnected. However, the different material properties of Cu compared to Au, such as affinity to oxidation and hardness, mean that these insights cannot be directly transferred to Cu bonding processes. Thus, further research is necessary. This paper discusses a study of bonding interface formation under various bonding parameters. Cu wire was bonded on AlSiCu0.5 metallization and a bonding parameter optimization was carried out to identify useful parameter combinations. On the basis of this optimization, different samples were assembled using parameter combinations of low, medium and high US-power and bonding force. An interface analysis was subsequently carried out using shear testing and HNO_3 etching. Intermetallic phase growth was analyzed on cross sections of devices annealed at 200 °C for 168 h and 1000 h. Contacts bonded with low bonding force and high US-power tended towards cratering during shear testing. Bonding force proved to have a significant effect on intermetallic phase formation whereas US-power was found to exert only a minor influence. The intermetallic phase formation of annealed samples was analyzed using EDX and interpreted on the basis of phase formation kinetics. Three main intermetallic phases were identified.

1. Introduction

Cu is an alternative material to Au with lower costs, superior electrical and thermal conductivity, and higher mechanical strength. However, conventional Au ball/wedge wire bonding is still the most common interconnection technology used for microelectronic components. This is because Cu has an affinity to oxidation and work-hardening during the bonding process, which makes using inert gas during the flame-off process and well-defined and controlled bonding parameters necessary. Interface and specifically intermetallic phase (IMP) formation during bonding and diffusion mechanisms during annealing are important factors influencing the reliability of Cu contacts on AlSiCu chip metallization. Achieving a better understanding of bonding parameters and IMP formation in the contact interface is necessary as the two processes are closely interconnected. This paper presents the results of interface analyses on Cu ball/wedge contacts on AlSiCu0.5 chip metallization under various bonding parameters. Shear testing, cross section and topography measurement by confocal microscopy were used for interface analysis after bonding. SEM and EDX analysis of cross sections of annealed devices was carried out to analyze phase formation at 200 °C.

2. Experiments

The samples consisted of wire bonding test dies (10 mm × 10 mm) fully metallized with AlSiCu0.5 (1 μm thickness). Heraeus HC4 Cu wire, with a 25 μm diameter, approx. 13 cN breaking load and approx. 14% elongation, was used. The bonding tool employed was a SPT TS70-13-C-1/16-XL20DG on an ESEC 3088 bonder (120 kHz bonding frequency). The temperature of the substrate holder was set to 200 °C and the bonding time was set to 30 ms for all investigations and parameter combinations.

The first step of the experiments was an initial bonding parameter optimization for the experimental setup. US-power was varied in a range of 10 values. Bonding force (BF) was kept constant at 330 mN. The quality of the bonded contacts – deformation (mashed ball diameter after bonding (MBD) divided by wire diameter), contact symmetry, shear force and appearance of the sheared area after shear testing (shear mode) – were recorded for each US-power setting. A US-power setting was then selected from the

* Corresponding author.
E-mail address: stefan.schmitz@izm.fraunhofer.de (S. Schmitz).

0026-2714/$ - see front matter © 2010 Elsevier Ltd. All rights reserved.
doi:10.1016/j.microrel.2010.07.062

results and remained fixed in the second phase of the parameter optimization, in which the bonding force was varied. The mechanical strength of the bonding contacts was measured using shear testing. The shear height was set to 5 µm and the shear modes were defined as follows (visual appearance is shown in Fig. 1):

Shear mode 1: Crack in the Al/Cu interface
Shear mode 1*: Crack in the interface, metallization partially removed
Shear mode 2: Partial ball shear, remaining Cu socket <50% of contact area
Shear mode 3: Partial ball shear, remaining Cu socket >50% of contact area
Shear mode 4: Metallization lift-off
Shear mode 5: Cratering

Using the above optimized settings, six different parameter combinations (see Fig. 2) were selected by varying the bonding force and/or US-power. Six groups of samples were then assembled, one for each parameter combination.

To analyze the bonding interfaces the Cu ball contacts were removed using HNO_3 (concentration 65%). The contact region was analyzed using light microscopy and topography measurement (confocal microscopy). Furthermore, the bonded devices were annealed at 200 °C for 168 h and 1000 h to increase intermetallic phase (IMP) growth in the interface. This was then analyzed by means of SEM/EDX measurement of the cross sections.

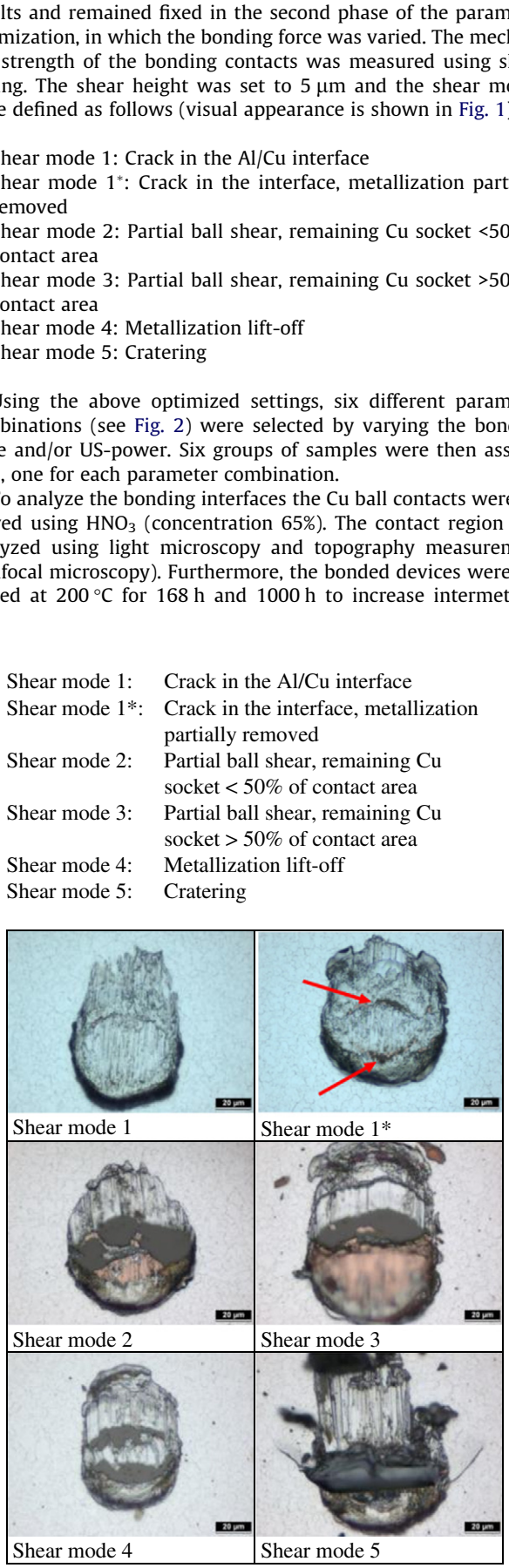

Fig. 1. Shear mode definitions.

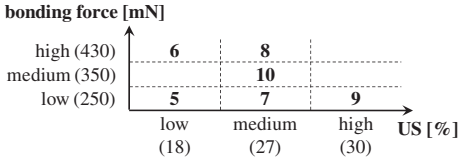

Fig. 2. Parameter combinations used for the experiments.

3. Results

3.1. Bonding parameter optimization

Table 1 and Fig. 3 summarize the results of the initial bonding parameter optimization. A high US-power setting of 30% clearly led to an increased amount of cratering (shear mode 5) and thus, this US-power level was defined as the maximum allowable setting for the experiments ("high" US-power). To effectively study the influence of the bonding force on cratering, a US-power value with some, but minimal, cratering (27%) was chosen ("medium" US-power). An US setting of 18% ("low" US-power) was chosen to study the effect of a parameter setting that is clearly to low. Table 2 and Fig. 4 show that bonding forces of $\geqslant$370 mN help prevent cratering during shear testing. Using these results the bonding parameters for the assembly of all samples used during the

Table 1
Results of US-power optimization.

US[a] (%)	Shear force (cN)	s.d. (cN)	Shear mode 1 + 1[a]	Shear mode 5	Shear strength (MPa)
18	39.6	1.7	30		104
22	54.1	1.9	29	1	133
23	57.4	1.9	28	2	136
24	58.3	1.6	30		136
25	61.6	1.6	30		143
26	66.1	2.3	29	1	147
27	69.4	2.0	29	1	151
28	72.2	2.3	29	1	155
29	73.3	2.6	30		155
30	77.6	2.4	24	6	162

[a] US-power is defined in % of the maximum energy output the ESEC wire bonder is set to.

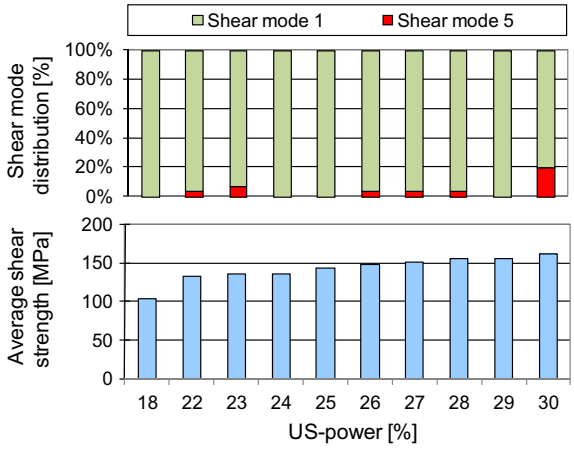

Fig. 3. Shear forces and shear modes at different US-power settings.

Table 2
Results of bonding force (BF) optimization.

BF (mN)	Shear force (cN)	s.d. (cN)	Shear mode 1 + 1*	Shear mode 5	Shear strength (MPa)
250	57.7	4.1	25	5	136
270	67.9	4.5	28	2	153
290	59.3	2.4	27	3	131
310	64.4	2.3	27	3	138
330	66.0	2.0	28	2	141
350	68.4	3.2	27	3	152
370	66.2	2.0	30		139
390	69.1	1.7	30		143
410	69.9	2.0	30		147
430	69.7	2.5	30		143

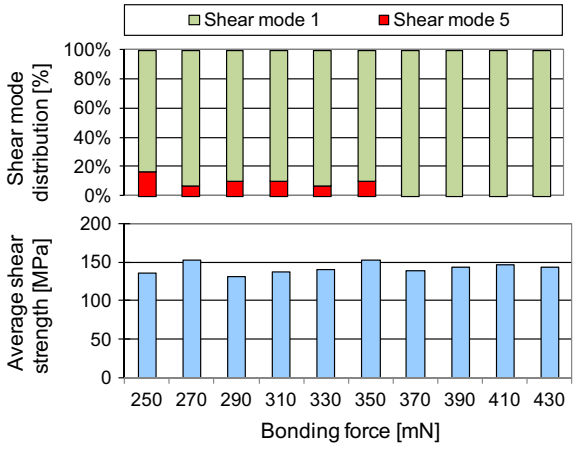

Fig. 4. Shear forces and modes at different bonding forces.

subsequent experiments (Fig. 2) could be defined. Table 3 summarizes the shear test results of the samples.

Sample 8 exhibited the highest shear strength (medium US-power and high bonding force). Sample 5, for which low bonding force and low US-power was used, showed the lowest shear strength of 93 MPa, which is approx. 42% lower than Sample 8. Low bonding force combined with high US-power appeared to lead to cratering (Sample 9), while Sample 10 bonded with medium bonding force and medium US-power showed approx. 60% less cratering. It is shown later (Fig. 11) that even high US only leads to very small interconnected areas. Eventually there is much energy and intrinsic stress stored in these regions that supports cratering. This must be analyzed further by FEM.

3.2. Influence of shear direction

The shear results discussed above were based on a shear direction parallel to the US vibration direction. Table 4 shows the results

Table 3
Shear test results of the bonding samples.

Sample No.	Shear force (cN)	s.d. (cN)	Shear mode 1 + 1*	Shear mode 5	Shear strength (MPa)	Shear strength* (MPa)
5	33.8	1.8	30		93	172
6	40.3	2.3	30		102	159
7	51.2	2.9	27	3	118	207
8	70.4	2.0	30		161	219
9	52.3	8.9	21	9	105	199
10	66.0	2.3	28	2	136	218

Shear strength* calculated based on the real interface area, see discussion and Fig. 7.

Table 4
Comparison of shear results in different directions.

Sample	Shear strength parallel to US direction (MPa)	Shear strength perpendicular to US direction (MPa)	Variation (%)
5	93	72	22.6
6	102	91	10.8
7	118	97	17.8
9	105	74	29.5

of a shear test experiment on Samples 5, 6, 7 and 9 using a shear direction perpendicular to the US vibration. In all cases, shearing perpendicular to the US vibration direction resulted in lower shear force values compared to the parallel shear direction. The variation ranged between 10% and 30%. When shearing parallel to the US vibration direction, the shear tool bent the loop and as a result the ball was pressed against the Al-Splash (see Fig. 6, Sample 5), which possibly produced a force component causing the increase in shear force and strength. This, however, needs further analysis, optionally using FEM simulation. The shear area after perpendicular shearing is shown in Fig. 5.

3.3. Interface analysis after HNO_3 etching of Cu

The remaining area after the shear test and the exposed interface region below the Cu ball after HNO_3 etching corresponded in size and appearance (Fig. 6). The interfaces of contacts bonded with medium and high US-power setting exhibited semi-circular regions where the Al metallization had been destroyed. In these regions, the Cu was in direct contact with the hard SiO_2 below the Al metallization. Due to the high mechanical stress generated by bonding force and US-power during the bonding process, the pad metallization can be considered an essential buffer zone, which decouples this stress from the brittle chip material. The partial destruction of the Al layer can have two negative effects:

- It increases the risk of cratering (confirmed by the results in Table 3, especially Sample 9).
- It leads to high inhomogeneities in the Al layer thickness, which can influence intermetallic phase growth and possibly contact reliability.

A low US-power setting (Samples 5 and 6) seemed to prevent this effect. HNO_3 etching of multiple Cu balls combined with visual inspection at minimum 200× magnification is an effective means of investigating the contact interface directly after bonding. The typical etching time at room temperature for contacts bonded with 25 µm wire (approx. 80 µm MBD) is 15 min, although the wires quickly dissolve (within 40–60 s). The higher etching rate of the wire compared to the ball is caused by the wire's much smaller grain size compared to that of the Cu ball after flame-off and bonding. Using an acid that mainly etches grain boundaries – such as HNO_3 in the case of copper – results in higher etching rates for volumes with a lot of small grains.

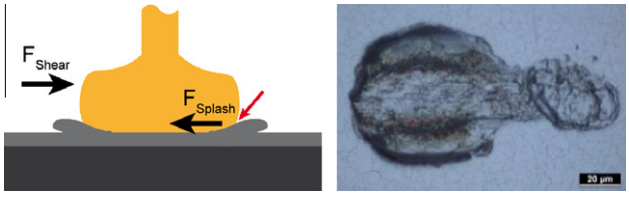

Fig. 5. Left: Shear force component generated by Al-Splash; Right: Shear area after perpendicular shearing.

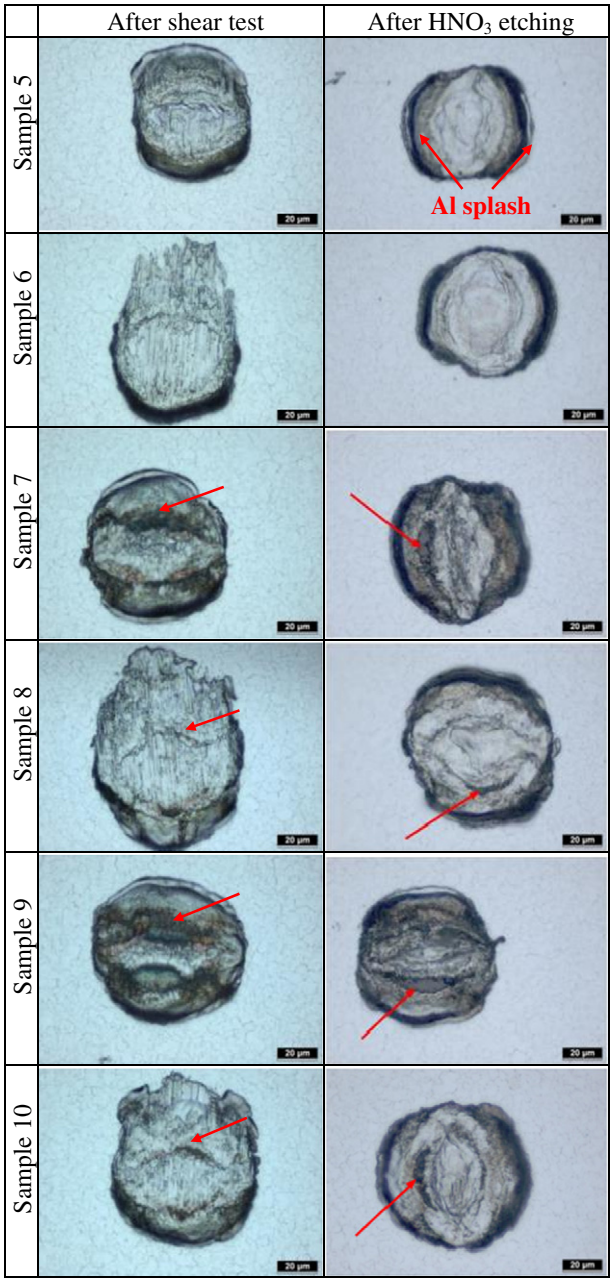

Fig. 6. Comparison of interface region below Cu ball after shear testing (left) and after HNO_3 etching (right).

3.4. Analysis of contact area

The interface contact area and symmetry of the Cu ball after HNO_3 etching can be measured using either light or confocal microscopy. However, light microscopy only provides a one-dimensional view of the top of the ball and interface and the bonded ball usually appears to also cover non-connected areas such as the Al-Splash, with the result that the calculated shear strength, typically calculated on the basis of the MBD, does not reflect the actual value. Confocal microscopy, on the other hand, is able to deliver topographic measurements and thus more accurate shear strengths can be calculated. Additionally, in confocal microscopy, software filtering of the measurements can differentiate between the heights of chip metallization, Al-Splash and interface. Depending on the capabilities of the software used, this could also be performed as a fully automatic process. However, in this study, the interface area was measured manually (Fig. 7) for each sample group. The results are clearly shown in Table 3, which compares the shear strengths based on both microscopy techniques (* denotes values based on confocal microscopy). Note that, for the values gained by confocal microscopy, the samples with partially destroyed Al metallization (7, 8, 9 and 10) have the highest values. Of these, Samples 7 and 9 (bonded using a low force setting) show the largest areas of destroyed Al metallization. In these destroyed regions, no significant shear strength was generated and the samples have slightly lower shear strength* values than Samples 8 and 10.

3.5. Shear test after temperature storage at 200°C

Shear test results after temperature storage for 168 h and 1000 h at 200 °C are summarized in Figs. 8 and 9. Higher temperatures result in accelerated interdiffusion of Al and Cu. These interdiffusion effects reduce microstructure defects and intrinsic stresses while promoting intermetallic phase growth. This leads to increased shear strength and is the reason for the shear mode shift observed after temperature storage. The shear mode mainly changed from a crack in the Al metallization (Shear mode 1) to a partial shear through the material of the Cu ball (Shear mode 2) after 168 h and to a metallization lift-off (Shear mode 4) after 1000 h. Shear strength values and distribution was nearly equal for both after 168 h and 1000 h. Compared to the initial state of the samples (Table 3), the occurence of cratering is much higher for both. This is largely a result of the higher shear strength during shear testing and the reduction of the Al "buffer layer" due to intermetallic phase growth. There was no indication during the experiments that the cratering was caused by pad damage during the bonding process.

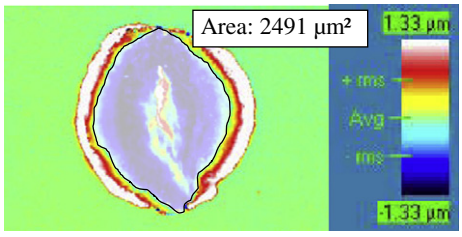

Fig. 7. Topography measurement of interface region.

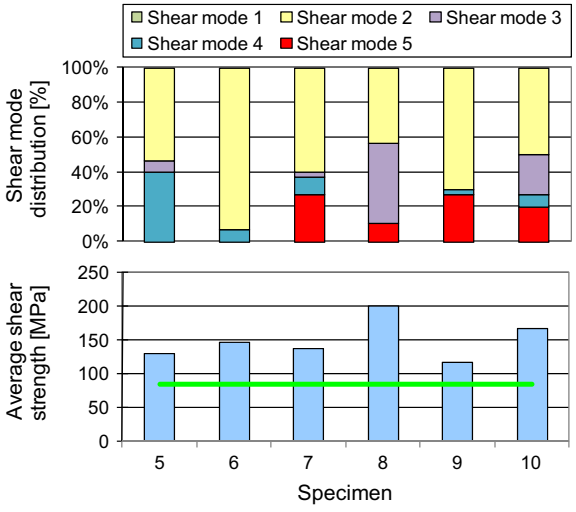

Fig. 8. Shear test results after 168 h storage at 200 °C.

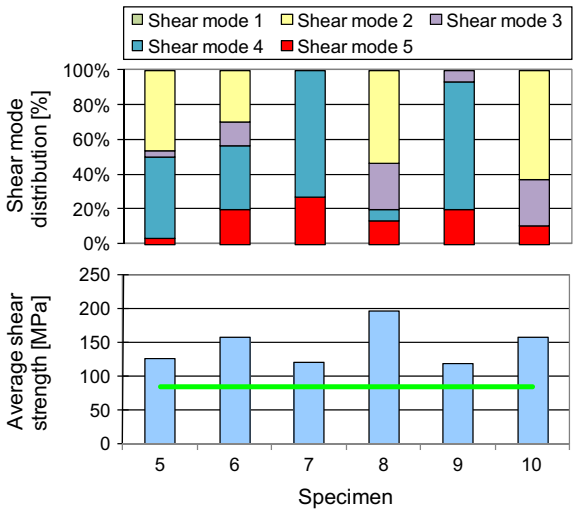

Fig. 9. Shear test results after 1000 h storage at 200 °C.

3.6. Intermetallic phase analysis

Cross sections of the samples stored for 168 h at 200 °C were analyzed by SEM and EDX (Figs. 10–12). Areas with IMP are marked in red. At a constant US-power of 27%, an increase of the bonding force led to a more uniform lateral distribution of the IMP (Fig. 10). An increase of the US-power at a constant bonding force (Fig. 11) did not seem to have a significant effect on IMP distribution in the interface. Notably, no IMP is visible at the edges of the interface, although the US-power of Sample 9 was nearly double that of Sample 5. Since high US-power increases the risk of damaging the Al metallization in the interface (Fig. 6) and high bonding forces can prevent cratering (Fig. 4) and support uniform IMP formation in the interface, we hypothesized that low US-power combined with high bonding force represents an optimized parameter combination for Cu bonding on AlSiCu metallization. This assumption was confirmed by the interface analysis on Sample 6 (Fig. 12), to which this parameter combination was applied. High bonding forces supports cold hardening, the generation of dislocations and point defects in the bonding interface. This supports diffusion processes and therefore the forming of IMP. Ultrasound causes reorganization of point defects and therefore possibly influences diffusion. This needs to be analyzed further.

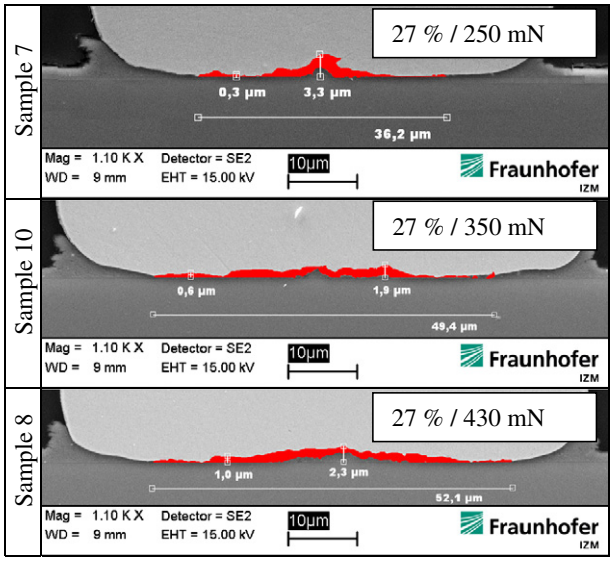

Fig. 10. Influence of bonding force on IMP coverage.

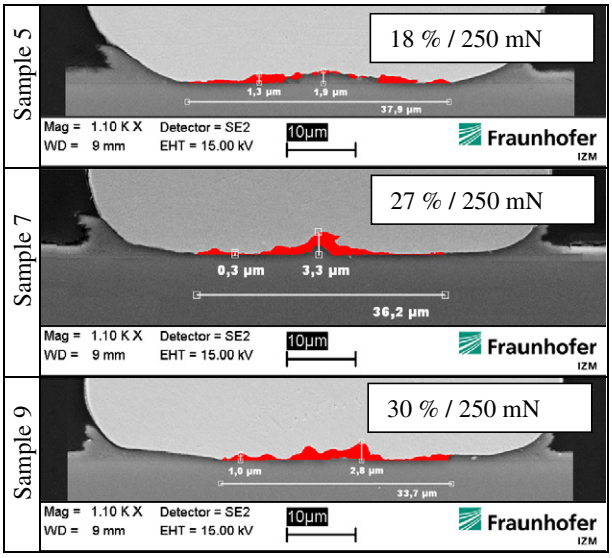

Fig. 11. Influence of US-power on IMP coverage.

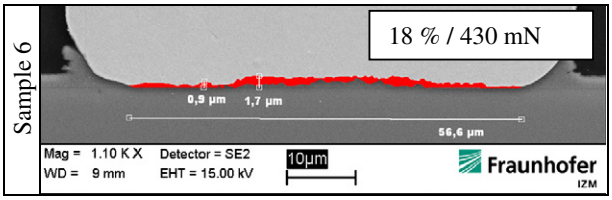

Fig. 12. Most uniform IMP coverage for low US-power and high bonding force.

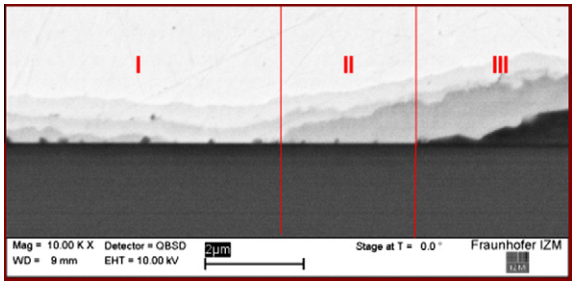

Fig. 13. Three regions of IMP growth (168 h @ 200 °C).

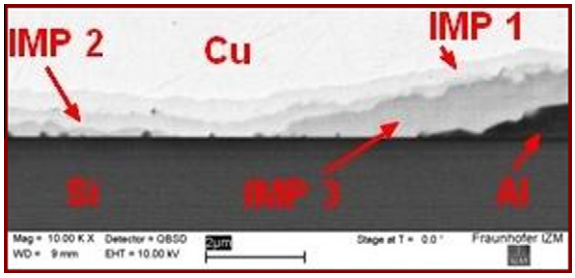

Fig. 14. IMP formation after 168 h at 200 °C.

Five stable IMP were identified in the Cu/Al-System. These IMP are either formed directly from the alloyed materials (Al and Cu in

this case) or the existing IMP is transformed into a new IMP. Both processes can include a transitional IMP (instable IMP). The effects are also temperature dependant, as shown for thin film samples in [1,2] where a $CuAl_2$ IMP was directly formed from Al/Cu at 130 °C, and have been confirmed in [3]. Additionally, it is assumed that a thin transitional IMP (β-Cu_3Al) is formed between Cu and $CuAl_2$ at a temperature of 170 °C. Subsequently, at temperatures of 200 °C and above, the IMP growth is influenced by the amount of Al. With only a little Al available, the β-Cu_3Al phase is transformed into the Cu_9Al_4 phase at the Cu-rich side. In this process Cu is set free and in combination with $CuAl_2$ a CuAl phase is formed between the β-Cu_3Al- and $CuAl_2$ phase. The resulting IMP-layer stack is a build-up of $CuAl_2$/CuAl/β-Cu_3Al/Cu_9Al_4/Cu. If the Al is fully exhausted the IMP-layer stack is built up from CuAl/Cu_9Al_4/Cu. These IMP formation processes become much more complex with greater amounts of Al but, since a pad metallization can be considered a small amount of Al, this does not have to be discussed further. The SEM image in Fig. 13 shows 3 regions of IMP growth. The left region (I), in which the Al has been undergoing transformation for a long time, the middle region (II), in which Al transformation has just been completed and right region (III), in which Al is still available. Based on the kinetics of phase formation, region III consists of a thick Al_2Cu phase, a CuAl phase and a Cu_9Al_4 phase. According to the literature, the β-Cu_3Al phase is very thin and for this reason it cannot be visually discerned. With no more Al available in region II the $CuAl_2$ phase decreases because of the growth of the two other IMP. In region I the Al is used up and the $CuAl_2$ phase is almost fully transformed; thus the layer stack comprises CuAl/Cu_9Al_4/Cu. Following this reasoning, the final state Cu_9Al_4/Cu should be reached after a longer storage period at 200 °C, although this was not confirmed within the duration of our study.

An EDX measurement of the cross section shown in Fig. 14 identifies the three IMP as:

- IMP1: Cu_9Al_4
- IMP2: CuAl
- IMP3: $CuAl_2$

4. Summary

This research project analyzed the interface formation during Cu ball/wedge wire bonding on AlSiCu0.5 chip metallization subjected to various bonding parameters. A bonding parameter optimization was carried out to identify potential parameter ranges. On the basis of this optimization, six groups of samples were assembled using parameter combinations of low, medium and high US-power and bonding force. An interface analysis was then carried out using shear testing and HNO_3 etching. The IMP growth was analyzed on cross sections of devices annealed at 200 °C for 168 h and 1000 h.

The most frequent failure mode during shear testing after bonding was a crack in the interface Cu/Al. Typically this shear mode is characterized by a closed metallization without visible areas below the bonding pad. On samples with different shear mode appearance it was demonstrated that the Al metallization had been destroyed during the bonding process due to high US-power or low bonding force. Bonding parameters were shown to affect IMP formation on devices annealed at 200 °C for 168 h. An increased bonding force led to a better IMP distribution in the interface. US-power variation was not found to significantly affect IMP formation. High bonding forces in combination with low US-power led to an optimized IMP coverage. SEM and EDX analysis identified three IMP: Cu_9Al_4, CuAl and $CuAl_2$.

References

[1] Zschech E. Bondkontakte. Berlin: Akademie-Verlag; 1990.
[2] Vandenberg JM, Hamm RA. An in situ X-ray study of phase formation in Cu–Al thin film couples. Thin Solid Films 1982;97:S313–323.
[3] Pretorius R, Vredenberg AM, Saris FW. Prediction of phase formation sequence and phase stability in binary metal–aluminium thin-film systems using the effective heat of formation rule. J Appl Phys 1991;70:S3636–3646.